SAND94-0606C
CONF-941012--1

Atomic Oxygen Interaction With Nickel Multilayer and Antimony Oxide Doped MoS_2 Films *

Michael T. Dugger, *Sandia National Laboratories, Albuquerque, NM 87185-0340*

Abstract

Sputtered MoS_2 is a solid lubricant capable of ultralow friction coefficients (below 0.05) and high load-bearing capacity. Since it exhibits low friction in vacuum, low outgassing rate, is non-migrating and lacks organic binders, this material is an attractive lubricant for space mechanisms. To exploit these new materials to their fullest potential, designers of space-based motion systems require data on the effects of atomic oxygen exposure on dense, sputtered MoS_2. This paper describes the effects of atomic oxygen in low earth orbit on the friction and surface composition of sputtered MoS_2 films. Sputtered multilayer films of MoS_2 with nickel (0.7 nm Ni per 10 nm MoS_2, for 1 μm total film thickness), and MoS_2 cosputtered with antimony oxide (nominally 2 μm thick) were exposed to 2.2 to 2.5×10^{20} oxygen/cm^2 over a period of 42.25 hours in earth orbit on the United States space shuttle. Identical specimens were kept as controls in desiccated storage for the duration of the mission, and another set was exposed to an equivalent fluence of atomic oxygen in the laboratory. The friction coefficient in air and vacuum, and the composition of worn surfaces, were determined prior to the shuttle flight and again after the shuttle flight. Delamination of the nickel multilayer film occurred on specimens exposed to shuttle flight. As-deposited and worn surfaces contained a greater atomic fraction of sulfur than molybdenum. Exposure to atomic oxygen caused a reduction in the atom fractions of carbon and sulfur, and an increase in oxygen. Despite dramatic changes in surface composition, sputtered MoS_2 films that did not delaminate retained their excellent tribological properties. This is attributed to confinement of the reactions with atomic oxygen to the near-surface region, protecting the bulk of the film from oxidative degradation. During sliding, the oxidized material was worn away, exposing the underlying MoS_2, which developed a surface composition identical to that of the as-deposited and worn material. Lubricated surfaces exposed continuously to atomic oxygen while in motion are expected to exhibit higher friction coefficients and wear rates than those shielded from atomic oxygen, or those exposed to atomic oxygen while static. Differences in material response between flight-exposed and ground-exposed specimens were attributed to thermal cycling which occurs during flight exposure. Silica contamination deposited on specimens exposed to atomic oxygen in low earth orbit acted as a barrier to oxidative degradation, suggesting that intentionally-deposited layers of silica may be used to protect sputtered MoS_2 lubricants from oxidation in low earth orbit prior to use.

HH

* This work was performed at Sandia National Laboratories, which is supported by the U.S. Department of Energy under contract number DE-AC04-94AL85000.

Introduction

Spacecraft mechanisms may encounter environments which include temperatures from cryogenic to several hundred degrees Kelvin, pressures from atmospheric to hard vacuum, and exposure to ultraviolet radiation and reactive species in the upper ionosphere. These operating conditions frequently preclude the use of liquid lubricants. At low earth orbit (LEO) altitudes of 200 to 1000 km, the primary species present is atomic oxygen [Leger et. al 1986], at pressures of less than $\sim 10^{-5}$ Pa. Although the atomic oxygen density is rather low, spacecraft orbital velocities of ~8 km/s result in a flux density on exposed surfaces of 10^{13} to 10^{15} atoms/cm^2·s, with a mean kinetic energy of approximately 5 eV/atom [Leger and Dufrane 1987]. The degradation of organic materials under these conditions is well known [Leger et. al 1985]. Solid lubricants with organic binders are therefore not appropriate for applications requiring long term exposure to atomic oxygen. Sputtered films of MoS_2 are attractive lubricants for these applications since no binders are employed. They have the additional advantage that films on the order of 1 μm thick exhibit low friction and low frictional noise. Thin lubricating films with low frictional noise are required for application in cryogenic devices, precision pointing mechanisms and components having high dimensional precision [Roberts 1990].

The interaction of sputtered MoS_2 with atomic oxygen has been investigated by a number of authors [Martin et. al 1989, Cross et. al 1990, Arita et. al 1992]. Martin and coworkers [Martin et. al 1989] exposed rf sputter-deposited nanocrystalline MoS_2 films and single-crystal MoS_2 to 1.5 eV atomic oxygen from a laser-sustained plasma source. Oxide layers 10-30 monolayers thick were found to form in the near-surface region, and consisted primarily of MoO_3 with a small amount of MoO_2. Oxide thickness was independent of crystallographic orientation of the MoS_2, and the authors found that the oxide layer had a low diffusion rate for oxygen. Compared to oxidation in humid air, which is dependent on the crystalline structure of the films, the authors discovered that atomic oxygen bypassed the dissociative chemisorption step so that the reactivity was insensitive to crystallographic orientation. Cross et. al [1990] examined the gaseous reaction products of sputtered and single crystal MoS_2 with atomic oxygen. They found that SO_2 outgassed from the surface during exposure. They also found that there was no translational activation energy barrier for the reaction, i.e., that atomic oxygen with thermal energies reacted with MoS_2 as readily as that having 1.5 eV translational energy. The authors also observed a high initial friction coefficient (0.25) on the MoS_2 film exposed to the hyperthermal atomic oxygen beam. The oxidized layer was removed by wear within the first 25 contact cycles. More recently, Arita and coworkers [1992] examined the friction and surface composition of a range of solid lubricant materials exposed to an atomic oxygen beam with a mean translational energy of approximately

5 eV. The authors found that irradiated films of sputtered MoS_2, inorganic-bonded and organic-bonded MoS_2, and ion-plated Pb had initial friction coefficients that were 20 to 30 percent higher than non-irradiated films. Composition profiling in the films revealed that the oxide layer varied in thickness from 6 nm for sputtered MoS_2 to 69 nm for the inorganic-bonded sprayed MoS_2 films.

Several advances have been made in recent years to increase the density of sputtered MoS_2 films, thereby reducing their vulnerability to oxidative degradation [Lince 1990]. These include operating at lower gas pressures [Aubert et. al 1990, Nabot et. al 1990], concurrent ion bombardment during film growth [Bolster et. al 1991], and periodic passivation of active growth sites with metallic interlayers [Hilton et. al 1992]. Modern sputtered films are amenable to a degree of compositional and microstructural control that was not possible with early sputtered films, and they possess concomitant improvements in performance. However, interaction of these structurally-modified materials with atomic oxygen has not been examined. In addition, due to the difficulty of performing experiments in the LEO environment, all of the published information on the interaction of MoS_2 with atomic oxygen has been obtained under laboratory conditions. The purpose of this investigation was to determine the effects of hyperthermal atomic oxygen exposure on the tribological performance and surface composition of structurally-modified sputtered MoS_2 thin films. The materials examined in this work were nickel multilayer and antimony oxide-doped MoS_2 films. Atomic oxygen exposures were performed aboard the United States space shuttle and at a ground-based LEO simulation facility, to provide a comparison between the actual LEO environment and laboratory atomic oxygen exposure.

Experimental

A. Materials Preparation

Substrates for sputtered MoS_2 deposition were 440C stainless steel. Disks were parted from 2.53 cm diameter bar stock to a thickness of 0.13 mm. The substrates were then heat treated to maximum hardness (58-62 Rockwell C) using a 788 °C preheat for 30 minutes, austenitized at 1038 °C for 50 minutes, oil quenched, then tempered at 163 °C for 60 minutes. Thermal treatments were conducted with substrates sealed in quartz tubes and separated by glass wool. The tubes were evacuated and backfilled with dry argon (dew point $\leq$ -55°C) to reduce oxidation. The substrates were then parallel-lapped and polished using standard metallographic techniques to an arithmetic surface roughness (R_a) of $\leq$20 nm. Control numbers were etched on the back of samples so that the specimens could be tracked and uniquely identified throughout coating, space flight, and analysis, should they become separated from their numbered containers. The disks were cleaned ultrasonically in acetone followed by isopropanol,

rinsed in deionized water, and blown dry with nitrogen. Substrates were sealed in PTFE containers and stored in a desiccator until the lubricant was deposited.

MoS_2 films were sputtered on the 440C disks by sources that use radio frequency (rf) magnetron sputtering [Hilton et. al 1992] and DC sputtering [Stupp 1981]. Disks were sputter cleaned prior to deposition of the coatings to remove atmospheric contaminants and oxide layers, in order to promote film adhesion. Nickel multilayer films were deposited by rf magnetron sputtering using one metal target and one MoS_2 target. The specimens were mounted vertically on a platform that rotates about the vertical axis of the chamber, and was used to move the substrates in front of the targets alternately to deposit layers of nickel and MoS_2 [Hilton et. al 1992]. A 5 nm interfacial layer of nickel was first deposited on the 440C surface, followed by alternate layers of MoS_2 (10 nm) and Ni (0.7 nm). A total of 95 layers were deposited, and the layered structure was given a 50 nm top coat of pure MoS_2. Antimony oxide doped films were deposited by DC triode sputtering from a composite target. The target was composed of pressed MoS_2 powder and contained 30 wt.% Sb_2O_3 powder. The films were nominally 2 μm thick. Figure 1 illustrates the structure of the two types of specimens investigated. All films were deposited between June and July of 1991.

Several sets of disk specimens were produced, so that comparisons between LEO and laboratory atomic oxygen exposure could be made. Group A specimens were exposed to atomic oxygen in LEO. Group C specimens were exposed to atomic oxygen in a laboratory simulation of the LEO environment. Group D specimens were controls that were not exposed to atomic oxygen, and were kept in a desiccator while the other groups were processed. There were two identical specimens in each group. One specimen was used for pre-flight friction tests under laboratory air ambient conditions, and the other for pre-flight friction tests in vacuum (less than 10^{-6} Pa). Post-flight tests in both of the ambient environments were performed on each of the specimens. All the MoS_2 films of a given film type were deposited simultaneously in the same deposition run. Table 1 shows the specimen designations, exposure conditions, and test conditions for the specimens.

The counterface for tribological evaluation was a 440C stainless steel, hemispherically-tipped pin. Pins were cut to length from 1.58 mm diameter rod, and a hemispherical cap with 0.79 mm radius of curvature was machined on one end. Heat treatment, polishing and cleaning of the pins was identical to that for the disk substrates. The pins were not coated.

B. Pre-flight Characterization

Prior to flight, group A specimens were subjected to pin-on-disk friction tests and surface analysis using Auger electron spectroscopy (AES) and x-ray photoelectron spectroscopy (XPS). Friction tests were performed using a vacuum flange-based pin-on-disk tribometer [McDonald et. al 1987] with an applied normal load of 35 gf and a sliding speed of 2±1 cm/s for 1000 disk revolutions, or cycles. The applied load resulted in a peak Hertzian contact stress of 1.1 GPa. Tests were performed in both ambient laboratory air (23±2°C and 35-55% relative humidity) and vacuum (pressure $\leq 1\times10^{-6}$ Pa). For pre-flight characterization, only two tests were performed in each environment in order to conserve space on the disks for post-flight analysis.

After friction tests in vacuum, the worn surface composition was determined using AES without removing the test device from the vacuum chamber. The surface compositional data were therefore not compromised by exposure to air between friction testing and surface analysis. Surface compositional analysis was performed by rastering the electron beam (10 kV, 5 nA, 35 nm diameter) over an area approximately 40 μm × 40 μm in size. Wear track widths were typically on the order of 100 μm wide for tests in vacuum, and wider for tests in air. The composition data reported for worn surfaces therefore included no contribution from the unworn material adjacent to the wear track. A rastered electron beam was used for two reasons. First, early analyses comparing rastered beams with stationary beams revealed that even for beam currents as low as 1 nA, beam damage could be detected as relative intensity shifts in the sulfur, molybdenum, carbon and oxygen peaks, as a function of analysis time. Second, a rastered beam results in a more accurate representation of the nominal surface composition, since the effects of local microscopic inhomogeneities were averaged out. The electron beam parameters chosen were found to yield adequate signal-to-noise ratios in reasonable analysis times without inducing any changes in composition due to beam damage. Compositional analysis was performed at three locations on each wear track, both inside and outside the track, for a total of 6 areas.

C. LEO Atomic Oxygen Exposure

The specimens were shipped to the Jet Propulsion Laboratory for integration into a specimen tray. All of the flight-exposed, ground-exposed, and control specimens were photographed and analyzed using XPS, then weighed (after 24 hours conditioning in a 50% relative humidity, room temperature chamber). The specimens were then subjected to a thermal vacuum conditioning treatment by heating to 65°C for 62 hours in vacuum, in accordance with NASA Johnson Space Center (JSC) requirements. Post-thermal-vacuum XPS results on ultra-clean optics in the same thermal treatment batch as the solid lubricants indicated 1-2 nm of hydrocarbon accumulation as a result of the outgassing treatment, which should be

removed with $< 10^{17}$ oxygen/cm^2. This amount of hydrocarbon accumulation was therefore considered to be negligible. Group D specimens were placed in a desiccator for storage until flight and ground exposure of the other specimen groups was complete.

The specimen tray consisted of a plate containing 2.22 cm diameter "windows" (for the 2.53 cm diameter specimens). The coated surface of the specimen faced the window in the plate, and the specimen was held against the plate with a wavy washer and a backing plate. Further details of the specimen-to-tray and tray-to-pallet integration for subsequent space flight exposure are presented in the reference by Chung and coworkers [1993].

The group A specimens were exposed to atomic oxygen in low earth orbit aboard NASA's Evaluation of Oxygen Interactions with Materials Experiment-3 (EOIM-3). The EOIM-3 pallet was included in space shuttle mission STS-46 aboard the shuttle Atlantis, launched July 31, 1992. The STS-46 mission included the European Retrievable Carrier (EURECA) satellite and the Tethered Satellite System (TSS-1) as primary payloads, and the Thermal Energy Management Processes Experiment (TEMP 2A-3) and EOIM-3 as secondary experiments. After deployment of the EURECA satellite at a Mission Elapsed Time (MET) of 1 day, 17 hours and 8 minutes (01/17:08), Atlantis kept a station-keeping orbit with the satellite, providing approximately 4 hours of atomic oxygen exposure to the EOIM-3 pallet at an altitude of approximately 425 km. At MET 05/22:30, with Atlantis in a circular orbit of 230 km and the payload bay oriented into the orbital velocity vector, the bay doors were opened to begin the EOIM-3 atomic oxygen exposure experiment. The shuttle maintained the ram attitude (with the normal to the payload bay parallel to the velocity vector) ±20° until MET 07/16:45, providing a total elapsed exposure time of 42.25 hours. The atomic oxygen fluence for EOIM-3 was estimated to be 2.2 to 2.5×10^{20} atoms/cm^2, based on atmospheric modeling, erosion of on-board Kapton films, and measurement by an on-board mass spectrometer.

The pallet also experienced an estimated 22 equivalent solar hours (±20%) UV exposure. Twelve temperature sensors included on the EOIM-3 pallet provided an estimate of the thermal history of the tray during the mission. During EURECA deployment, the shuttle maintained a solar inertial attitude for about 12 hours. The tray (and the more massive specimens on the tray) reached a temperature of +55°C during this period. The temperature reached another peak of about 32°C during TSS-1 satellite deployment. Temperatures cycled between about +5°C and +20°C during the EOIM-3 exposure period.

The EOIM-3 pallet was removed from Atlantis on August 15, 1992 and the tray containing the solid lubricants for this study was returned to JPL on August 27, 1992. After de-integration and post-flight

analysis at JPL, samples were returned to investigators for analysis. Further details on specimen handling and a summary of results for other materials on the EOIM-3 tray are presented in the reference by Chung and coworkers [1993].

D. Ground-Based Atomic Oxygen Exposure

Group C specimens were exposed to atomic oxygen in a ground-based facility that uses a pulsed molecular beam valve, coupled to a conical nozzle and a 14 J/pulse CO_2 laser [Chung et. al 1993]. Briefly, the pulsed valve allows a burst of gas into the conical nozzle. A laser pulse directed into the cone and heats the gas to > 20,000 K. The plasma expands into the diverging cone and cools, forming a beam of fast neutral atoms with a small fraction of ionic and molecular components, traveling at hyperthermal velocities. Source conditions were adjusted to maintain a mean oxygen atom velocity of 7.8 km/s, with a velocity distribution similar to that in LEO. An $O:O_2$ ratio of about 4, total ionic content of one percent, and UV radiance of about one photon per 10^4 incident oxygen atoms has been measured for this source. Specimens were placed 50 cm from the source, so that heating through energy accommodation of the hyperthermal atoms or scattered laser radiation was negligible.

The batch of EOIM-3 specimens containing the solid lubricants for this study experienced an atomic oxygen fluence (determined by the weight loss of four Kapton witness specimens with reactivity 3.00×10^{-24} cm^3/atom) of 1.97×10^{20} atoms/cm^2, with a mean velocity of 7.8 km/s. The exposure duration was 25.28 hours. Additional details on the ground-based exposure facility can be found in the reference by Chung and coworkers [1993], and references therein.

E. Post-flight Analysis

Sample evaluation after flight was identical to that performed before flight, as described above. In this case, all friction tests were repeated at least three times at each test condition. Worn surface composition data were again obtained at three locations on each wear track, so that post-flight composition data represents the combined results from nine separate areas for each test condition. Pre- and post-flight XPS data were acquired, but in the present paper only the friction and Auger data are reported.

Results and Discussion

A. Morphology and Tribology

The morphology of the Ni/MoS_2 and MoS_2+SbO_x films after exposure to atomic oxygen in low earth orbit is shown in Figure 2. The low magnification image in Figure 2(a) indicates that the Ni/MoS_2 film experienced large-scale delamination, with the film cracked and curled up away from the substrate over

much of the exposed surface. The curvature of the film suggests a tensile stress at the film surface with respect to the film/substrate interface. Kustas [1993] also observed delamination of multilayer films ($AuPd/MoS_2$) after exposure to atomic oxygen in a plasma asher. Polishing scratches in the substrate were visible through the film. Although most of the film surface was damaged, adherent areas could be found, and were generally smooth and featureless, as shown in Figure 2(b). The ground-exposed and control specimens of Ni/MoS_2 showed no indications of film cracking or delamination, and appeared as in Figure 2(b) over the entire disk surface. The only visible change in the ground-exposed surface relative to the control specimen was a slight change in contrast in the exposed central region of the disk. The outer rim of the disk that was protected from atomic oxygen by the mounting plate was visible to the naked eye, as well as in the electron microscope. Since the exposure levels for atomic oxygen were similar for the flight-exposed and ground-exposed surfaces (about 2.3 and 2.0×10^{20} atoms/cm^2, respectively), the film cracking and delamination is probably the result of factors other than atomic oxygen in the flight environment. The most obvious difference was the thermal cycling which occurred in the flight ambient, but not during the ground exposure. However, the temperature change for most of the cycling was modest (about 15°C), and there were a total of only about 50 cycles after the last temperature peak during TSS-1 deployment. As will be shown later (and has been established by previous authors), the oxidized region of the films was confined to the upper ~10 nm, so that migration of the oxygen 0.99 μm through the nickel layers to attack the interface is unlikely. Auger analysis in a region where the film had completely spalled off, revealing the substrate, indicated a surface composition of 3.5 at.% S, 3.6% Mo, 41.6% C, 32.7% O, 12.5% Fe and 6% Ni. The major species present excluding atmospheric contaminants (C, O) was iron, suggesting that delamination occurred at the substrate/nickel interface. The Mo and S levels reported are near the background noise level in this energy region, and may be due to fine debris distributed over the analysis area. These films will be composition profiled when other analyses are complete, to shed more light on this issue.

The morphology of the flight-exposed MoS_2+SbO_x film is shown in Figures 2(c) and 2(d). This material also exhibited a change in contrast in the exposed region of the disk relative to the periphery, which was protected by the sample mount. No film cracking or delamination was observed on any specimens of this type. The texture seen in Figure 2(d) is characteristic of the deposition process, since it appeared on all specimens regardless of exposure history. The particulate features near the center of Figure 2(d) also appeared on all specimen surfaces, and have the same composition as the film away from these features. They may be foreign particles imbedded in the film, or large particles from the target deposited at the film surface.

The friction coefficient versus disk revolutions, or cycles, is shown in Figure 3 for a test in laboratory air on the ground-exposed Ni/MoS_2 film. This figure illustrates the features seen in friction tests, and how the various test attributes have been defined. The specimens exposed to atomic oxygen exhibited a large initial friction coefficient, μ_i, at the beginning of the test. The peak friction coefficient was a factor of 2 to 10 greater than the final, steady-state value, μ_f. The run-in period for atomic oxygen exposed Ni/MoS_2 films varied from 40 to several hundred cycles, while that for MoS_2+SbO_x films was typically 30 cycles or less. As-deposited and control groups exhibited no significant period of run-in. Large initial friction coefficients for atomic oxygen-exposed MoS_2 have been observed by other researchers [Martin et. al 1989, Cross et. al 1990, Arita et. al 1992], and are attributed to wear and displacement of the oxidized surface layer to expose unoxidized material below.

Figure 4 shows the final friction coefficient μ_f as a function of specimen exposure conditions. The high μ_f values in air for the Ni/MoS_2 film tested in the as-deposited, control and flight-exposed conditions shown in Figure 4(a) are a result of film failure and metal/metal wear during these tests. The final friction coefficient for the ground-exposed specimen in air was 0.18, and did not exhibit film failure. This behavior may be due to differences in the degree of sputter cleaning prior to film deposition, and hence to the thickness of the oxide at the film/substrate interface, between the specimens in this deposition run. The fact that the film failure observed on as-deposited and flight-exposed specimens occurred both before and after flight supports this conclusion. The μ_f values for tests in vacuum on this material indicated much lower friction coefficients than in air. Lubricant film delamination due to atomic oxygen exposure was observed only for the flight-exposed specimen, and even in this case redistribution of the lubricant and transfer film formation resulted in a μ_f of 0.08 in vacuum.

Final friction coefficients for the MoS_2+SbO_x specimens are shown in Figure 4(b). The final friction values exhibited essentially no change from the as-deposited to atomic oxygen exposed conditions, with μ_f values in air near 0.10, and those in vacuum near 0.02. The friction coefficient for the control specimen was significantly higher than that for the other specimens of this material, in both air and vacuum ambients. This was attributed to large levels of surface contamination on this specimen, as discussed below.

B. Composition

Post-flight XPS performed at JPL revealed a small amount of silicon on all flight samples. The geometry of a visible deposit on a polycrystalline diamond film was used to estimate that the contamination source was in the aft portion of the orbiter, not more than 30° above the plane of the tray.

Materials on the EOIM-3 pallet easily eroded by atomic oxygen contained 2-3 atom percent silicon, while more stable materials contained 9 to 12 atom percent silicon. Possible sources of the silicon are a silicone-based waterproofing agent applied to the shuttle's thermal protection system tiles, or an insulation blanket treated with silicone oil that covers the aft bulkhead.

Figure 5 illustrates the changes observed in Auger spectra of the unworn films as a result of atomic oxygen exposure. Spectra for the control, flight-exposed and ground-exposed Ni/MoS_2 films are shown in Figure 5(a). The figure indicates that exposure to atomic oxygen resulted in a reduction in surface carbon and sulfur. The erosion of carbon in hyperthermal atomic oxygen is well documented [Leger et. al 1985]. Cross and coworkers [1990] found that SO_2 was also generated and outgassed from sputtered MoS_2 surfaces in a 1.5 eV atomic oxygen beam. The depletion of carbon and sulfur observed in the present work is consistent with those results. The unworn surface of the flight-exposed specimen exhibited a significant amount of silicon contamination. The position of the Si_{LMM} Auger transition suggests that the silicon was present as SiO_2. The absence of prominent sulfur or molybdenum peaks in this spectrum was due to masking by the layer of silicon contamination, and suggests that the layer was more than about 3 nm thick. Figure 5(b) shows Auger spectra acquired on unworn surfaces of the control, flight-exposed and ground-exposed MoS_2+SbO_x films. Atomic oxygen exposure resulted in depletion of the surface sulfur and carbon on this film, as for the Ni/MoS_2 film. The increase in the peak-to-peak height for antimony after atomic oxygen exposure suggests that the oxide phase in the MoS_2+SbO_x film resisted etching by atomic oxygen, and its concentration at the surface increased as carbon and sulfur were removed as gaseous oxidation products.

The peak-to-peak heights from Auger spectra like those shown in Figure 5, combined with published sensitivity factors [Davis et. al 1979], were used to create the atomic concentration charts shown in Figures 6 and 7. Figure 6 shows the atom fraction of each detected species on the Ni/MoS_2 film surface as a function of exposure and tribological test conditions. The open bars represent data from the unworn surface, the cross-hatched bars correspond to the air worn surface, and the solid bars show atom fraction data from the vacuum worn surface. Error bars are shown only for the unworn data to demonstrate the uncertainty in the composition information, and improve the clarity of the figure. Figure 7 shows the equivalent data for the MoS_2+SbO_x film. Figures 6(c) and 7(c) are included to illustrate the composition of wear surfaces created *before* the shuttle flight, and then exposed to atomic oxygen in low earth orbit, relative to the unworn and LEO-exposed surface. The bars indicating unworn surface composition in Figures (c) and (d) therefore represent the same data.

Unworn Surfaces

Figures 6(a) and 6(b) show that the unworn surface (open bars) composition of the Ni/MoS_2 film increased in carbon and oxygen after desiccator storage for approximately two years, compared to the as-deposited film. The sulfur concentration decreased on the control surface, which became nearly 1:1 in S:Mo compared to 2:1 in the as-deposited film. The flight-exposed surface became about 20 at.% silicon and 45 at.% oxygen, as shown in Figure 6(c) and 6(d). Atomic oxygen reduced the surface sulfur to about 3 at.%, and the S:Mo ratio became approximately 1:2. Carbon contamination on the flight-exposed surfaces was reduced, due to reaction with atomic oxygen to produce volatile reaction products. Figure 6(e) shows that the ground-exposed surface exhibited changes from the as-received and control specimens similar to those observed for the flight-exposed specimens, except that the silicon contamination layer was absent on the ground-exposed specimen. Carbon concentration was reduced and surface sulfur was depleted, producing a S:Mo ratio of about 1:2.5. Iron was also absent on the unworn ground-exposed specimen due to the absence of film cracking to expose the substrate.

Figure 7(a) shows that the as-deposited surface of the MoS_2+SbO_x film was very rich in sulfur, with a S:Mo of about 4:1. The antimony dopant was present at about 8 at.%, compared to approximately 30 at.% in the sputtering target used to deposit the films. The oxygen content was near 10 at.%, similar to the Ni/MoS_2 specimens. The control surface reflected very high carbon levels, on the order of 65 at.% as shown in Figure 7(b). The S:Mo ratio also changed to about 2:1 compared to the as-deposited surface. No iron was observed on any of the MoS_2+SbO_x specimens, in worn or unworn locations, indicating that the film remained intact and adherent. The flight-exposed surface exhibited a decrease in S:Mo relative to the unexposed surfaces, to about 1:3. This was accompanied by a dramatic increase in the oxygen content to 45 at.%. The O:Sb ratio remained near 1.5:1, which implies that the oxide was not removed by erosion. A decrease in the carbon concentration to 18 at.% in this specimen was the result of reaction with atomic oxygen to form volatile reaction products. Silicon was present at about 5 at.%. The ground-exposed specimens showed similar effects, as seen in Figure 7(e). The S:Mo ratio changed to about 1:3, and the carbon contamination layer reduced to near 15 at.%. The silicon contamination layer was absent from the ground-exposed specimen, and the concentration of oxygen at the surface was higher (about 50 at.%) than that on the flight-exposed specimens as a result.

Comparison of Figures 6(a) and 7(a) reveals that the MoS_2+SbO_x surface was much richer in sulfur than the Ni/MoS_2 surface in the as-deposited condition. The volatility of sulfur oxidation products, and the higher sulfur concentration at the MoS_2+SbO_x surface, may explain the larger levels of silicon contamination observed on the Ni/MoS_2 film compared to the MoS_2+SbO_x film. As sulfur oxidizes and

volatilizes, deposited silicon contamination was also lost. Increasing silicon contamination levels on specimens having surfaces with greater oxidative stability was observed in other samples on the EIOM-3 tray [Chung et. al 1993].

Unexposed Worn Surfaces

Figure 6(a) shows that wear of the Ni/MoS_2 film in air caused a decrease in the atom fractions of sulfur and molybdenum relative to the unworn surface, but the S:Mo ratio remained approximately 2:1. Oxygen increased from 10 at.% to 35 at.%, and the presence of iron at 25 at.% suggests that the film has worn through to expose the substrate in some locations. Wear in vacuum caused no change in the carbon content from the unworn surface. The lack of iron suggests that the lower surface shear stresses on the film when sliding in vacuum, due to the lower friction coefficient, did not result in film delamination. This confirms the friction results. The S and Mo levels were similar to the unworn surface. The oxygen content on the vacuum worn surface was similar to that on the unworn surface, suggesting that some oxygen was present throughout the film. The composition after friction tests on the control surface, shown in Figure 6(b), indicated that wear in air produced increases in oxygen (45 at.%) and iron (20 at.%) relative to the unworn surface. The substrate was again exposed due to fracture of the coating under high shear stress in air. In vacuum, a dramatic reduction in the carbon and oxygen content within the wear scar was observed. The iron content was similar to the unworn surface in this case, implying that the low shear stress produced by sliding in vacuum did not damage the coating to the extent observed in air. A large increase in the sulfur content was observed after sliding in vacuum, producing a S:Mo ratio of 2.5:1. This behavior was similar to that observed on the as-deposited specimen.

Figure 7(a) shows that wear of the MoS_2+SbO_x film in air caused a slight increase in the sulfur content, with a decrease in antimony and oxygen. Wear in vacuum produced a surface composition essentially identical to the unworn case. No iron was observed in any wear rack, indicating that the film remained intact under the imposed shear stress. The control surface composition in Figure 7(b) showed that wear in air produced a slight increase in sulfur and a decrease in the carbon content, from 65 at.% on the unworn surface to about 55 at.% on the air worn surface. Relative amounts of other film constituents remained unchanged. When worn in vacuum (solid bars in Figure 7b), a decrease in carbon to 40 at.% was observed. The sulfur content increased to 35 at.%, giving a S:Mo ratio of 3:1 compared to 2:1 for the unworn and air worn surfaces. The surface contained much more carbon than the as-deposited specimen, while changes in the S:Mo and O:Sb ratios were similar.

Worn, Then Exposed Surfaces

Figure 6(c) illustrates the effect of wear prior to flight on the surface composition of the Ni/MoS_2 film after LEO atomic oxygen exposure. The surface worn in air prior to flight showed a dramatic change in the S:Mo ratio, from 2:1 before exposure (Figure 6a) to nearly 1:4 after exposure (Figure 6c), indicating a loss of sulfur. The surface worn in vacuum exhibited a similar change in the S:Mo ratio, from about 2.5:1 before exposure to 1:2 after exposure. Atomic oxygen exposed wear surfaces also exhibited a loss of carbon and an increase in oxygen relative to the non-exposed surfaces, just as for the unworn material. Silicon contamination also appeared on the exposed wear surfaces, as in the case of the unworn films. More silicon contamination appeared on the vacuum worn surface compared to the air worn surface. This may reflect differences in the erosion rate of these surfaces during atomic oxygen exposure. A higher erosion rate would result in less accumulated silicon contamination remaining at the end of the exposure. The MoS_2+SbO_x film worn in air and vacuum, and then exposed to atomic oxygen, exhibited virtually identical composition in the air worn and vacuum worn locations, as shown in Figure 7(c). The worn surfaces showed a change in S:Mo ratio from 4:1 before exposure (Figure 7a) to 1:3 after exposure (Figure 7c), indicating a loss of sulfur as observed for the Ni/MoS_2 sample. A dramatic increase was observed in the oxygen content, from about 10 at.% to 40 at.%. Figure 7(c) also shows that after wear followed by exposure, the concentration of all lubricant constituents (with the exception of oxygen) was lower than on the unworn surface, and the silicon concentration was higher. This suggests that the worn surfaces of MoS_2+SbO_x were more resistant to erosion by atomic oxygen than the unworn film, attributed to densification of the film during wear.

Exposed, Then Worn Surfaces

Auger analysis of the unworn Ni/MoS_2 film outside of wear locations was performed on regions that did not delaminate due to atomic oxygen exposure. Figure 6(d) shows that wear of the Ni/MoS_2 film in air removed the silicon contamination from the surface. Wear in air also caused the S:Mo ratio to increase to >1:1, compared to 1:2 on unworn surfaces. An increase in iron occurred after wear in air, reflecting removal of the film due to the combination of poor interfacial adhesion and high surface shear stress produced by sliding in air. The behavior of flight-exposed and ground-exposed surfaces was similar, with the exception that flight contaminants were completely absent from the ground-exposed surfaces as shown in Figure 6(e). Wear of flight-exposed surfaces in vacuum also decreased the silicon concentration. A large increase in the S:Mo ratio was observed for surfaces worn in vacuum, from <1:1 on unworn exposed surfaces to about 2.5:1 after wear on the flight-exposed and ground-exposed samples. There was a large reduction in the oxygen content after wear, indicating removal of the oxidized

material. The fact that the oxygen concentration remains high, while the silicon layer was removed on the flight-exposed specimen, suggests that the atomic oxygen penetrated the film, while silicon contamination resided at the surface. The amount of iron in the vacuum wear track increased to 3 at.% due to exposure of the substrate, but this was less than that observed in the wear track formed in air and was similar to the control specimen. Iron was absent from the vacuum-worn surface of the ground-exposed sample, since no film cracking was produced to expose the substrate prior to friction testing. The low friction coefficient exhibited by the film in vacuum also retarded the additional sliding-induced film removal which occurred in air.

Figure 7(d) indicates that friction tests in air of the MoS_2+SbO_x film caused complete removal of silicon on the flight-exposed specimen, attributed to wear of the coating. The S:Mo ratio increased from 1:3 on the unworn surface to 3:1 on air worn surfaces. The concentration of oxygen in the wear track decreased relative to molybdenum, compared to the unworn surface, suggesting wear of a surface oxidized layer. Silicon contamination remained on the flight-exposed surface worn in vacuum, indicative of a low wear rate in vacuum due to lower friction coefficients than in air. An increase in the S:Mo ratio to about 2:1 was observed after vacuum friction tests, similar to the surface worn in air. This observation is consistent with the tendency of MoS_2 to align basal planes parallel to the sliding direction, creating a sulfur-rich surface. The increase in C:Sb in the wear track relative to the unworn surface, particularly for wear tracks created in vacuum, indicates that carbon is distributed throughout the film, and not just present at the surface as atmospheric contamination. The ground-exposed surface (Figure 7e) worn in vacuum exhibited similar trends to the flight-exposed surface worn in vacuum. Flight contamination was absent from the ground-exposed surface, and the S:Mo ratio was somewhat higher, at nearly 4:1.

Thickness of the Reacted Layer

Peak height ratios for the low energy (S_{LVV} at 152 eV and Mo_{MNN} at 186 eV) and high energy (S_{KLL} at 2117 eV and Mo_{LMM} at 2044 eV) Auger transitions of sulfur and molybdenum were used to compare the thickness of the reacted layer on unworn surfaces, without performing destructive depth profiling. The electron beam was rastered over a rectangular area, as for the elemental surveys described above, but data was acquired only in the energy ranges of Auger transitions for elements present in the films. Selected peak height ratios are shown in Table 2. Based on the inelastic mean free path of electrons as a function of energy [Seah and Dench 1979], the sampling depth for the low energy peaks was about 2.6 nm (2σ, or 95% of electrons originate within 2.6 nm of the surface), while the sampling depth for the high energy peaks was about 8.8 nm. The change in S/Mo ratios for the low and high energy transitions,

relative to the S/Mo ratios on the control specimens, was calculated (Δ S/Mo in % = [$S/Mo_{CONTROL}$-$S/Mo_{EXPOSED}$]/$S/Mo_{CONTROL}$ × 100), and the results are shown in Table 3. The data show that for the lab atomic oxygen exposed specimens, the decrease in S/Mo ratio relative to the control surface at high energy was about half that seen at low energy. This result was similar to that seen by Martin et. al in their examination of single crystal and rf sputtered pure MoS_2 [Martin et. al 1989]. They also found that the oxide concentration decreased with depth in the MoS_2, dropping by a factor of two in the outer 9 nm. Atomic oxygen therefore penetrated the doped films examined in this study to the same level as single crystal MoS_2 and pure sputtered MoS_2. This was not surprising for the Ni/MoS_2 film, since it contains a 50 nm cap of pure sputtered MoS_2. The results for the MoS_2+SbO_x film indicated that the presence of antimony oxide did not significantly modify the reaction layer thickness. Comparison of the S/Mo reductions for the LEO exposed and lab exposed specimens indicates that the presence of the silicon flight contamination modified the interaction of the MoS_2 surfaces with atomic oxygen. The LEO exposed Ni/MoS_2 film experienced only about half the reduction in S/Mo at low energy that the lab exposed specimen did, and at high energy the S/Mo was essentially unchanged. This result suggests that the layer of SiO_2 formed on the Ni/MoS_2 surface *in situ* acted as a barrier to atomic oxygen penetration, and prevented oxidation of the lubricant to some degree. The S/Mo reduction at low energy for the MoS_2+SbO_x film exposed in LEO was also less than that observed on lab exposed surfaces, suggesting a protective effect of SiO_2 on this surface as well. Comparison of the reductions in S/Mo at the surface (low energy data) for the Ni/MoS_2 and MoS_2+SbO_x revealed different levels of protection for the two films. The data suggest that flight contamination provided more protection to the Ni/MoS_2 film than the MoS_2+SbO_x film. These results are consistent with the relative amounts of silicon contamination found after flight exposure of the two materials, as shown in Figures 6(d) and 7(d). The LEO exposed Ni/MoS_2 film contained about 20 at.% silicon on the unworn surface, compared with only about 5 at.% for the MoS_2+SbO_x film. The different levels of silicon contamination are attributed to different erosion rates for the two films in atomic oxygen - a higher erosion rate for the MoS_2+SbO_x would result in less accumulation of silicon contamination, and hence less protection from further exposure to atomic oxygen.

Summary and Conclusions

The surface morphology of flight-exposed and ground-exposed specimens exhibited some striking differences for the Ni/MoS_2 films. Although the flight-exposed specimens exhibited cracking and delamination of the film to expose the substrate, no such defects were found on the ground-exposed specimens. Since the cumulative oxygen doses for these two specimens were similar, the cracking and

delamination appeared to result from thermomechanical fatigue at the film/substrate interface. The ground-exposed specimens received no thermal cycling during exposure, while the flight-exposed specimens experienced thermal cycles at the orbital frequency of the shuttle. The differences in friction coefficient and surface composition between flight-exposed and ground-exposed samples are attributed to the differences in film cracking seen between these two sets of samples. Given these differences in morphology, friction and surface composition results were still similar for the flight-exposed and ground-exposed surfaces.

No differences in morphology were seen on the MoS_2+SbO_x specimens, because the film adhesion was sufficient to resist interfacial crack propagation due to differences in thermal expansion coefficient. Excellent correlation existed in friction and surface composition data between flight and ground-exposed specimens. In most cases, the differences in behavior were within the standard deviation of the measurements. Where there was deviation outside this range (some composition data), the difference was attributed to the lack of silicon flight contamination on the ground-exposed specimens.

The friction coefficient of the MoS_2+SbO_x solid lubricant film was insensitive to atomic oxygen exposure. Sliding in both air and vacuum produced surfaces which were sulfur-rich. Exposure to atomic oxygen caused loss of sulfur from worn and unworn regions, so that the films became sulfur-deficient and highly oxidized with respect to the starting material. This reaction layer was easily displaced during subsequent sliding, so that a steady-state friction coefficient identical to the unexposed material was produced. The composition of exposed surfaces also returned to one more typical of the as-deposited material after sliding for 1000 passes. Atomic oxygen appeared to penetrate the antimony oxide-doped MoS_2 more than the multilayer film, which may be due to increased porosity of the MoS_2+SbO_x coating. Antimony oxide did not significantly modify the thickness of the oxidized layer formed when exposed to atomic oxygen, compared to single crystal and pure sputtered MoS_2.

One area of concern regarding use of sputtered MoS_2 lubricants on surfaces exposed to atomic oxygen is accelerated wear rate. Volatilization of surface sulfur and oxidation to produce high friction coefficients will lead to an increase in the wear rate of the coating. For one-time applications such as deployment mechanisms, accelerated wear rate is of little consequence. Oxidation is confined to a thin surface layer, and the increase in startup friction can be accounted for in the design of the system. MoS_2-lubricated mechanisms continuously exposed to atomic oxygen, during continuous or repeated operation, will exhibit an accelerated wear rate. The effective life of the coating will be reduced, and the reduction will depend on the reaction rate of the film with atomic oxygen, the ratio of exposure time to duty cycle,

and the wear rate of the oxidized film. Additional work is necessary at a variety of dose levels to determine the reaction efficiency of sputtered MoS_2 with atomic oxygen.

The results of this study suggest that in addition to the oxidized layer formed when MoS_2 is exposed to atomic oxygen, a thin layer of silica (on the order of 3 nm thick) intentionally deposited over the sputtered MoS_2 prior to spacecraft deployment could be used to protect the lubricant from degradation while static.

Acknowledgments

The author wishes to thank Elizabeth Sorroche for performing the friction experiments and AES analysis. Enlightening discussions with Larry Pope, Jon Cross, and John Gregory were appreciated. Thanks to Shirley Chung at JPL for coordinating sample integration, and Lt. Col. Michael Obal for providing space on the EOIM-3 tray and for his support of the Space Environmental Effects (SEE) program by the Ballistic Missile Defense Organization (BMDO). Financial support from the Jet Propulsion Laboratory is gratefully acknowledged. This work was supported at Sandia National Laboratories by the U.S. Department of Energy under contract number DE-AC04-94AL85000.

References

1. L. Leger, J. Visentine and B. Santos-Mason, 18th International SAMPE Technical Conference 18, October 7-9, 1986, Seattle, Washington.
2. L. Leger and K. Dufrane, Proc. 21st AMS (1987), NASA Conf. Publ. 2470.
3. L. Leger, J. Visentine and J. Schliesing, 23rd Aerospace Sciences Meeting (1985), AIAA Paper 85-0476.
4. E. Roberts, Tribology International 23 (1990) 95-104.
5. J. Martin, J. Cross and L. Pope, Mat. Res. Soc. Symp. Proc. 140 (1989) 271-276.
6. J. Cross, J. Martin, L. Pope and S. Koontz, Surf. Coat. Technol. 42 (1990) 41-48.
7. M. Arita, Y. Yasuda, K. Kishi and N. Ohmae, Tribology Transactions 35 (1992) 374-380.
8. J. Lince, J. Mater. Res. 5 (1990) 218.
9. A. Aubert, J.-Ph. Nabot, J. Ernoult, and Ph. Renaux, Surf. Coat. Technol. 41 (1990) 127.
10. J.-Ph. Nabot, A. Aubert, R. Gillet, and Ph. Renaux, Surf. Coat. Technol. 43/44 (1990) 629.
11. R. Bolster, I. Singer, J. Wegand, S. Fayeulle, and C. Gossett, Surf. Coat. Technol. 46 (1991) 207.
12. M. Hilton, R. Bauer, S. Didziulis, M. Dugger, J. Keem, and J. Scholhamer, Surf. Coat. Technol. 53 (1992) 13.
13. B.C. Stupp, Thin Solid Films 84 (1981) 257.
14. T.G. McDonald, D.E. Peebles, L.E. Pope and H.C. Peebles, Rev. Sci. Instrum. 58 (1987) 593.
15. S.Y. Chung, D.E. Brinza, T.K. Minton, A.E. Stiegman, J.T. Kenny and R.H. Liang, Flight- and Ground- Test Correlation Study of BMDO SDS Materials: Phase I Report, Jet Propulsion Laboratory, California Institute of Technology, Pasadena, CA (JPL Pub. 93-31), 1993.
16. F.M. Kustas, Research and Evaluation of Atomic-Oxygen-Resistant Tribosurfaces, SBIR 92-1 Phase I Final Report, Contract No. NAS8-39800, Colorado Engineering Research Laboratory, Fort Collins, CO, 1993.
17. L.E. Davis, N.C. MacDonald, P.W. Palmberg, G.E. Riach and R.E. Weber, eds., Handbook of Auger Electron Spectroscopy, Physical Electronics Industries, Inc.: Eden Prairie, MN, 1976.

18. M.P. Seah and W.A. Dench, Surf. Interface Anal. 1, (1979) 2.

Table 1. Specimen Designation and Exposure Conditions

	LEO AO Exposed					
Film Type	**Pre-flight test, UHV**	**Pre-flight test, air**	**Lab AO Exposed**		**Control**	
Ni/MoS_2	1A	2A	1C	2C	1D	2D
MoS_2+SbO_x	3A	4A	3C	4C	3D	4D

Table 2. Peak Height Ratios for Auger Transitions of Film Constituents

Specimen	**S_{LVV}/Mo_{MNN} (152eV/186eV)**	**S_{KLL}/Mo_{LMM} (2117eV/2044eV)**	**O_{KLL}/Mo_{MNN} (510eV/186eV)**
Ni/MoS_2			
Control	3.20	1.03	3.98
LEO exposed	2.34	1.11	18.04
Lab exposed	1.38	0.73	5.61
MoS_2+SbO_x			
Control	8.32	1.27	4.80
LEO exposed	2.94	0.70	10.18
Lab exposed	1.58	0.81	9.19

Table 3. Change in S/Mo Peak Height Ratios Relative to Controls

Specimen	**Δ(S/Mo) from control (low energy)**	**Δ(S/Mo) from control (high energy)**
Ni/MoS_2		
LEO exposed	-27%	+8%
Lab exposed	-57%	-29%
MoS_2+SbO_x		
LEO exposed	-65%	-45%
Lab exposed	-81%	-36%

List of Figures

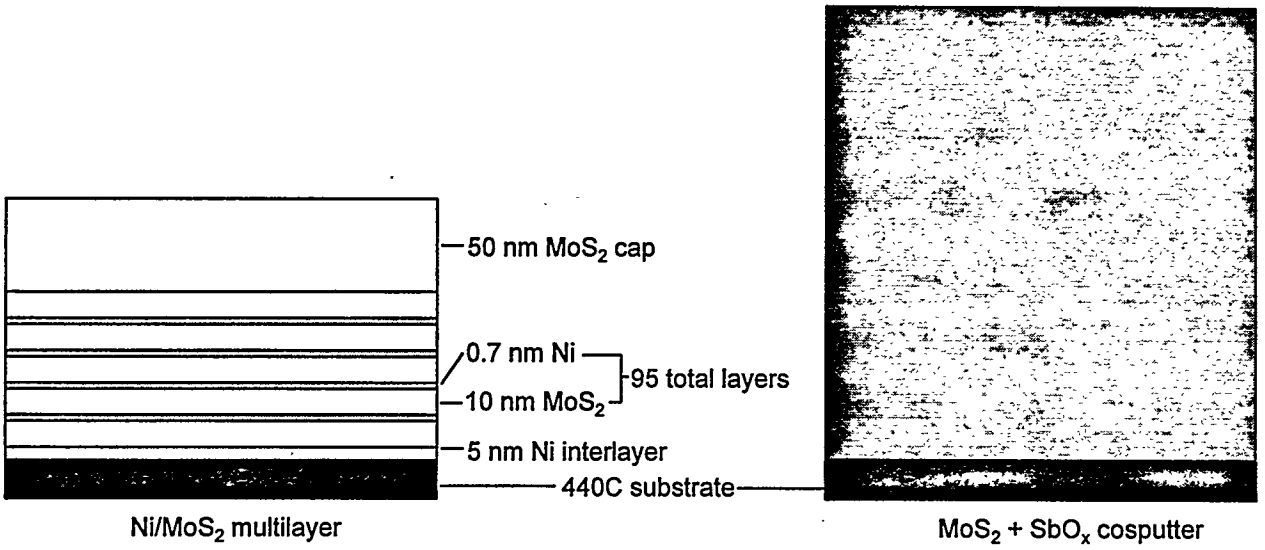
50 nm MoS_2 cap
0.7 nm Ni
95 total layers
10 nm MoS_2
5 nm Ni interlayer
440C substrate
Ni/MoS_2 multilayer
MoS_2 + SbO_x cosputter

Figure 1

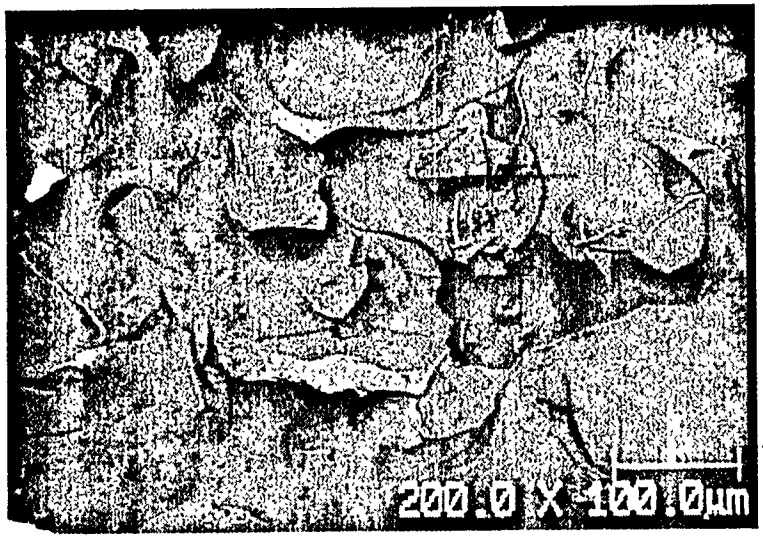

(a)

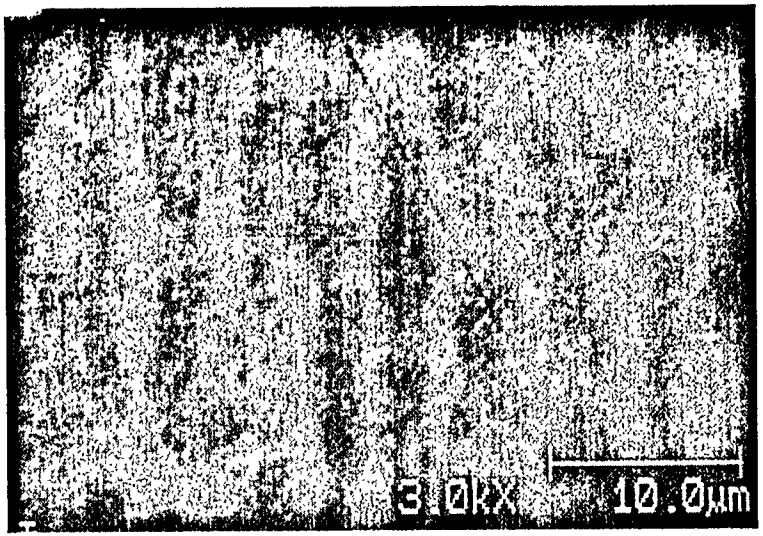

(b)

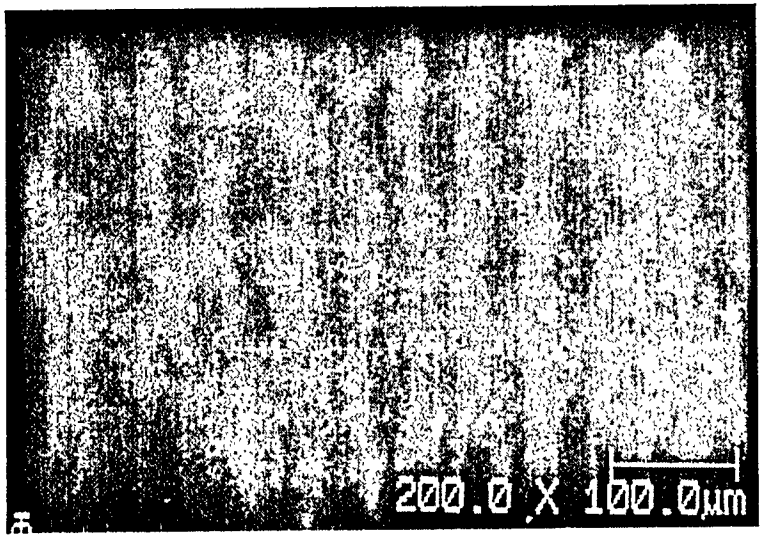

(c)

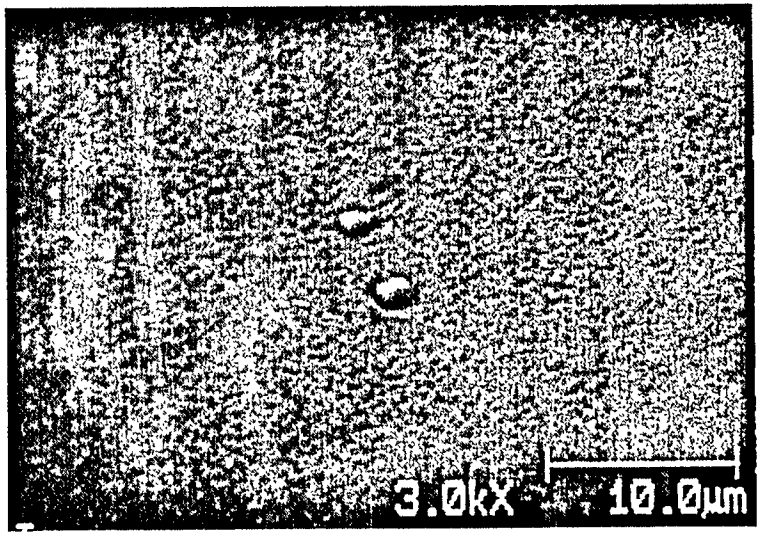

(d)

Figure 2

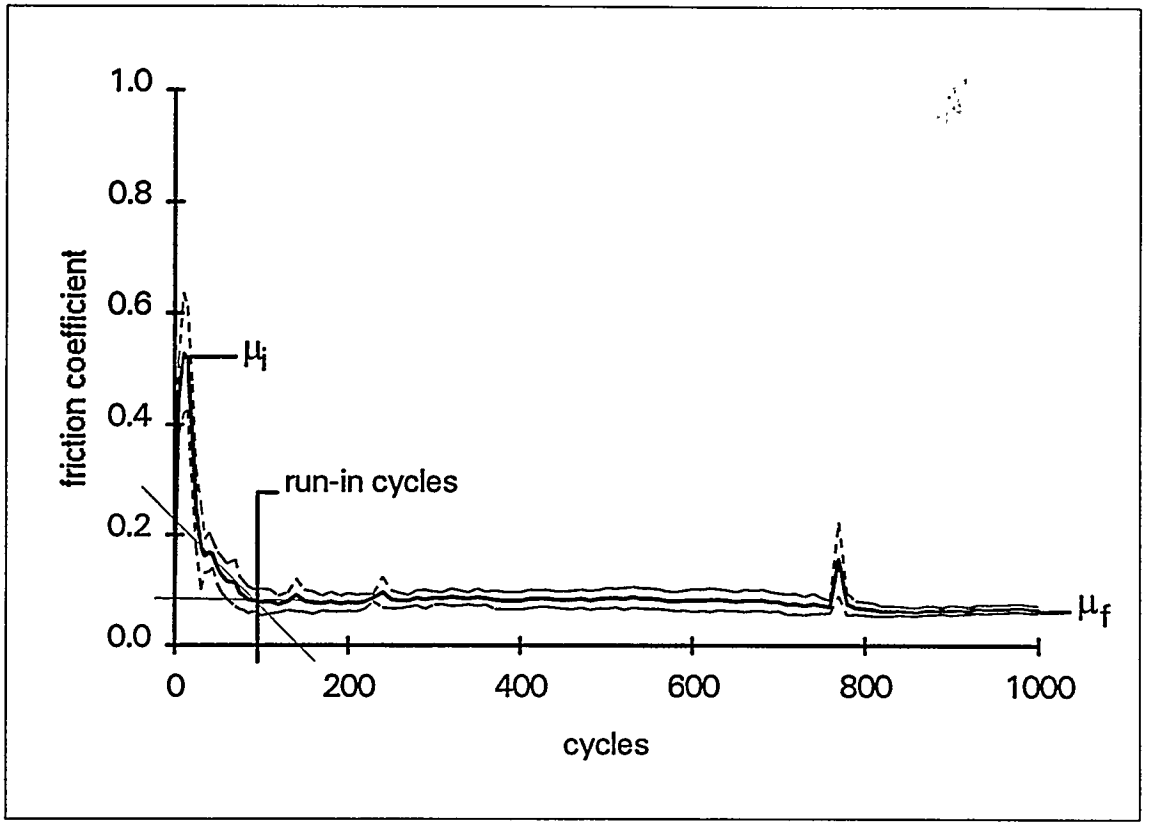
1.0
0.8
0.6
0.4
0.2
0.0
friction coefficient
μ_i
run-in cycles
μ_f
0
200
400
600
800
1000
cycles

Figure 3

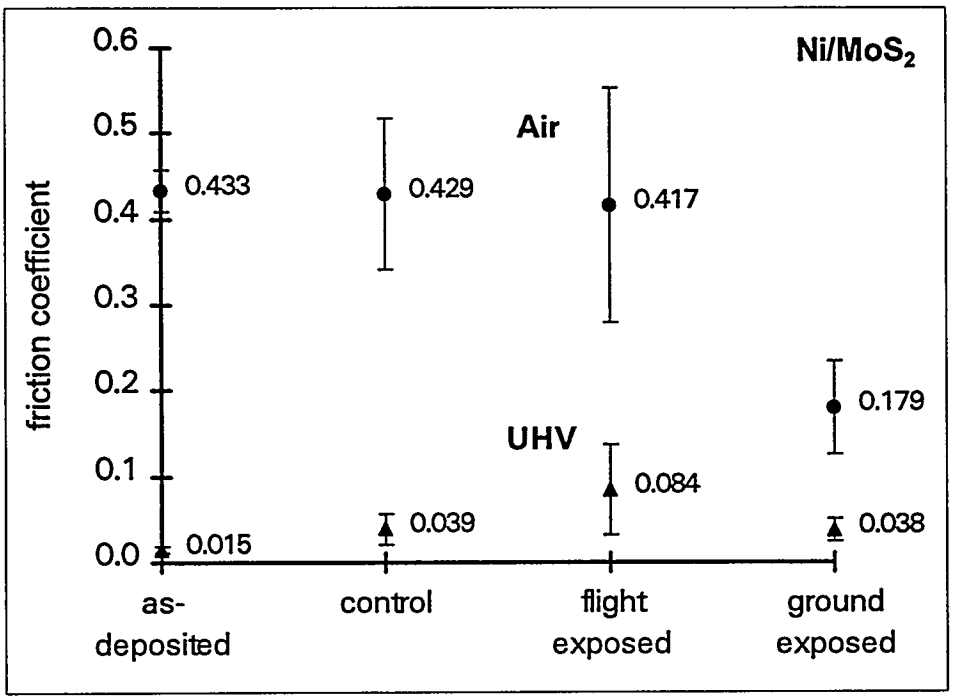
Ni/MoS2
friction coefficient
0.6
0.5
0.4
0.3
0.2
0.1
0.0
Air
UHV
0.433
0.429
0.417
0.179
0.084
0.039
0.038
0.015
as-deposited
control
flight exposed
ground exposed

(a)

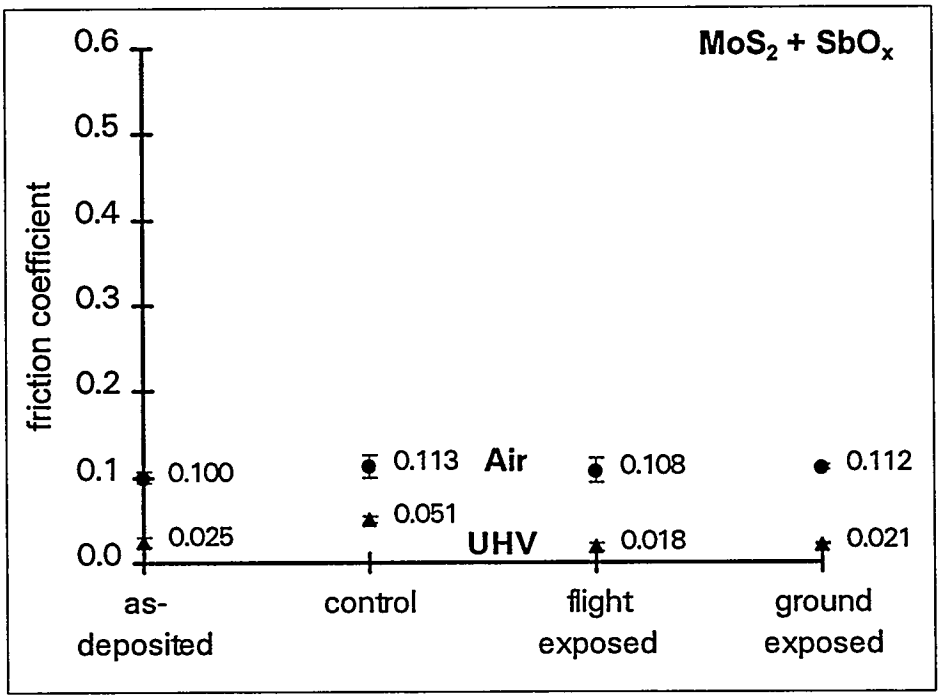
MoS2 + SbOx
friction coefficient
0.6
0.5
0.4
0.3
0.2
0.1
0.0
Air
UHV
0.100
0.113
0.108
0.112
0.051
0.025
0.018
0.021
as-deposited
control
flight exposed
ground exposed

(b)

Figure 4

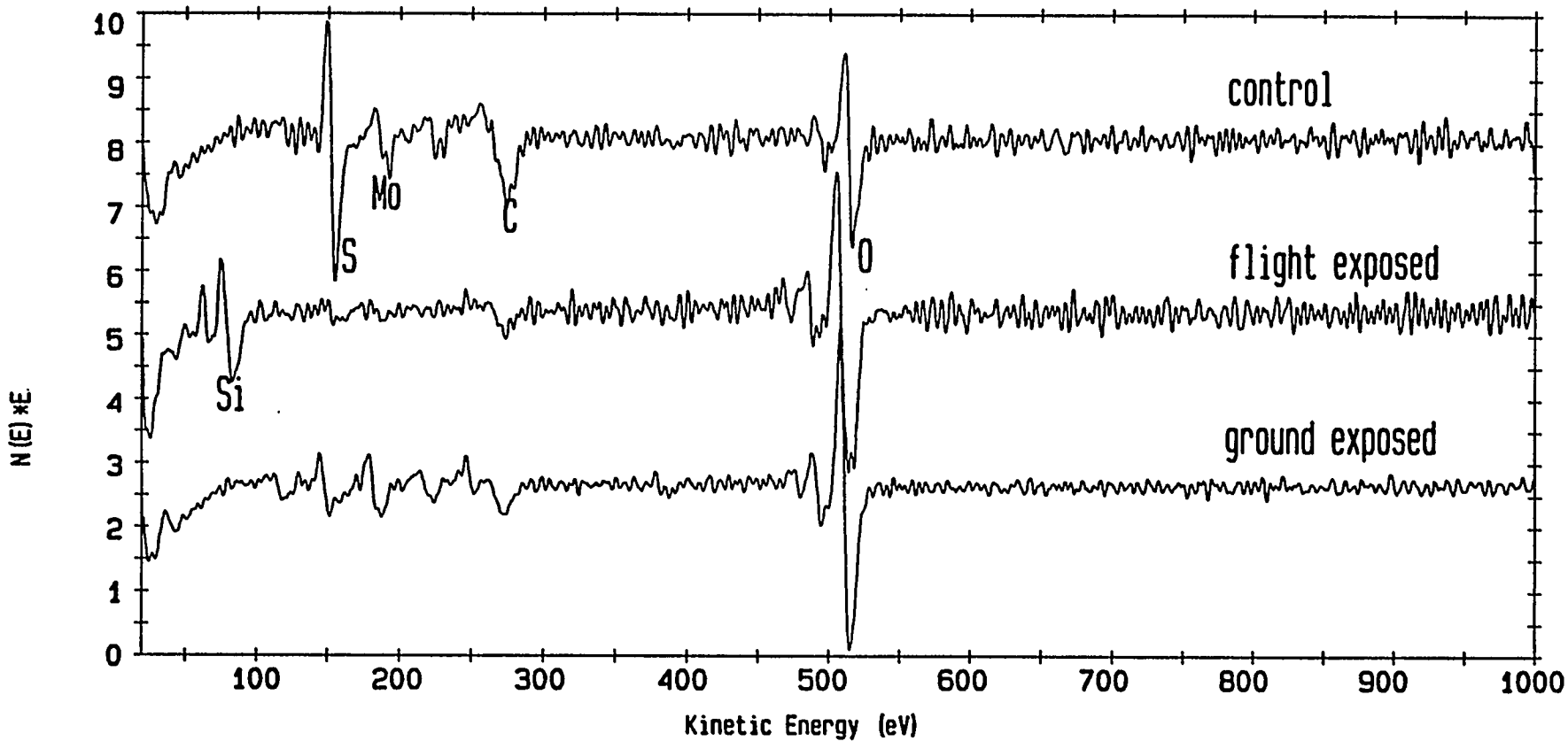
control
flight exposed
ground exposed
S
Mo
C
O
Si
N(E)*E
Kinetic Energy (eV)
0
1
2
3
4
5
6
7
8
9
10
100
200
300
400
500
600
700
800
900
1000

Figure 5(a)

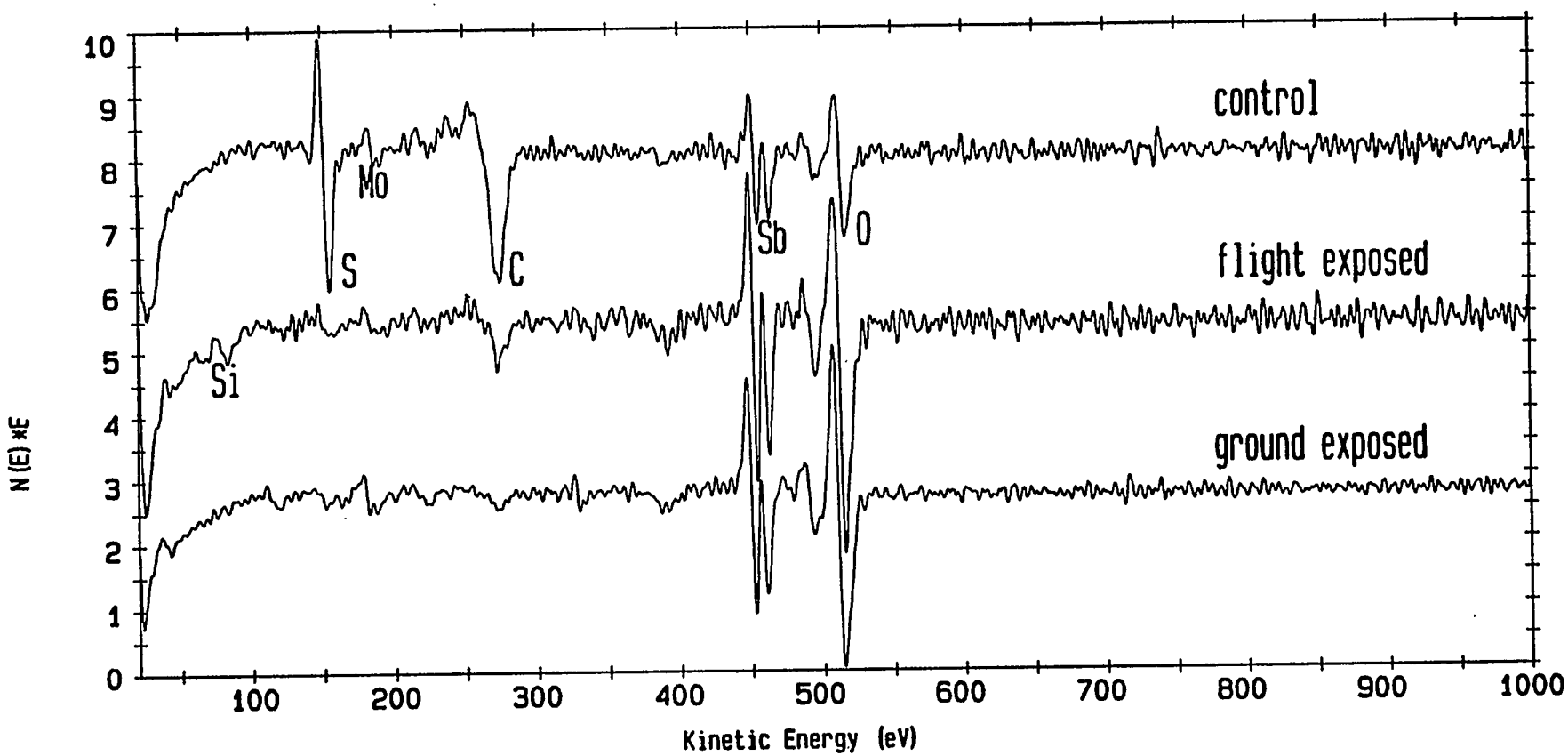
control
flight exposed
ground exposed
Mo
S
C
Si
Sb
O
N(E)*E
Kinetic Energy (eV)
0
1
2
3
4
5
6
7
8
9
10
100
200
300
400
500
600
700
800
900
1000

Figure 5(b)

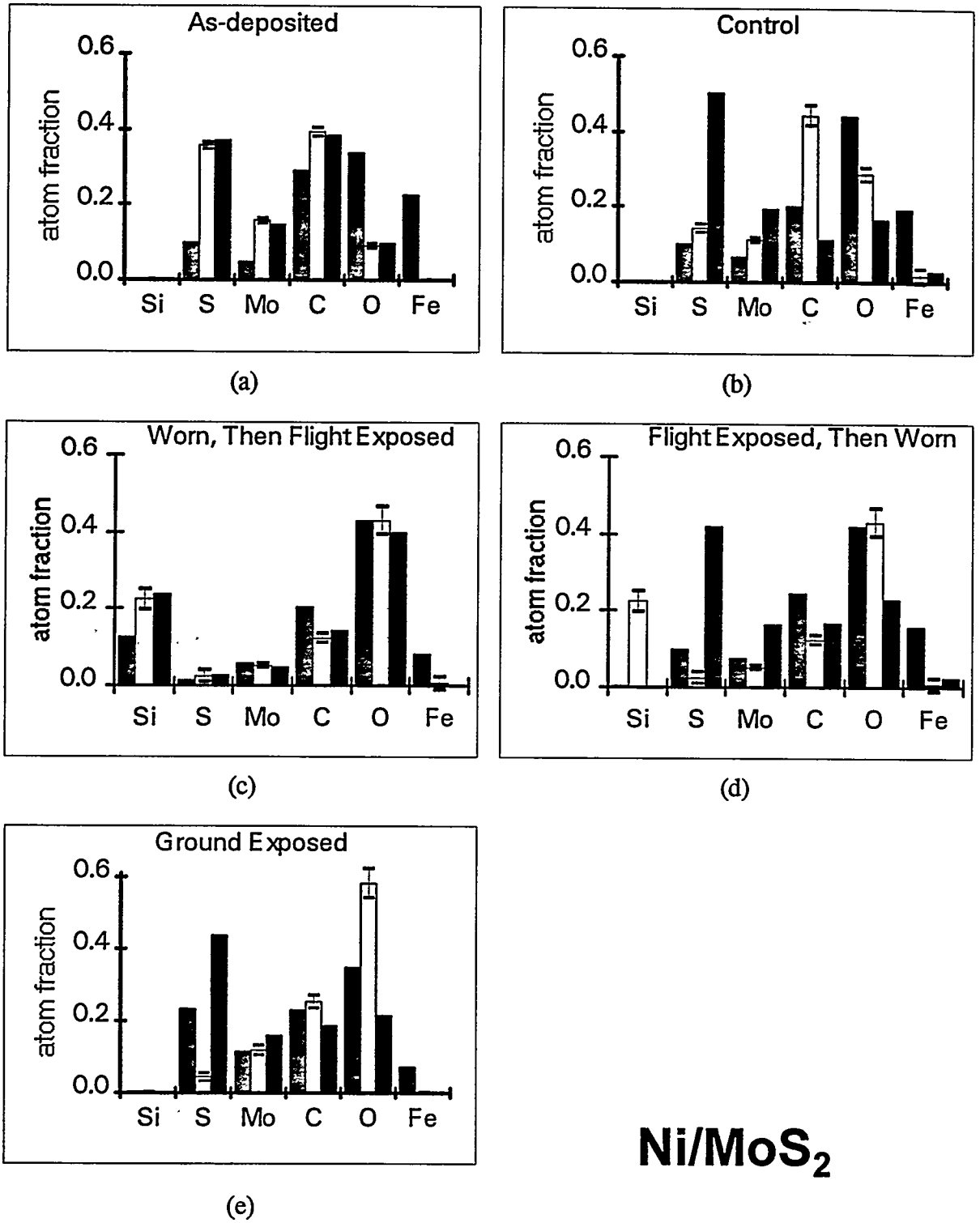
As-deposited
Control
Worn, Then Flight Exposed
Flight Exposed, Then Worn
Ground Exposed
atom fraction
0.6
0.4
0.2
0.0
Si S Mo C O Fe
(a)
(b)
(c)
(d)
(e)
Ni/MoS2

Figure 6

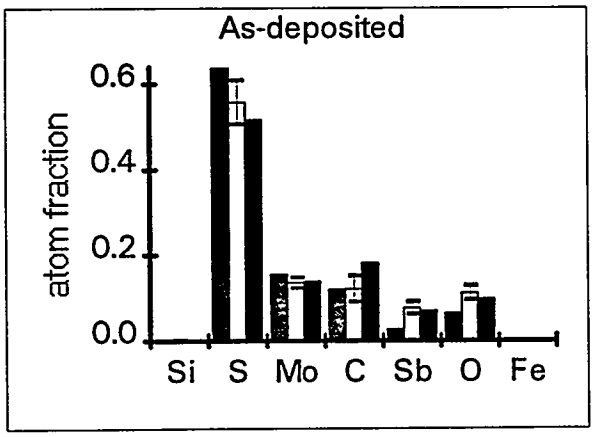

(a)

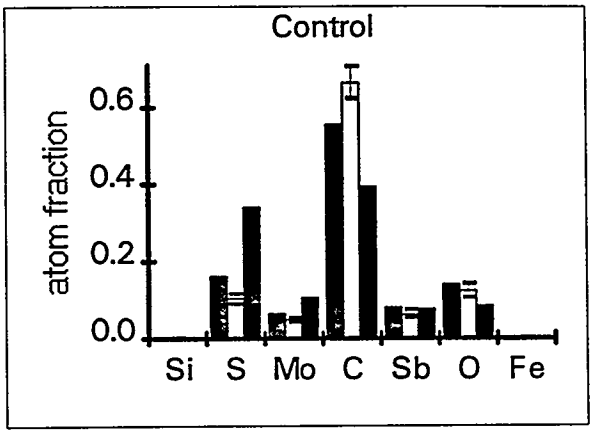

(b)

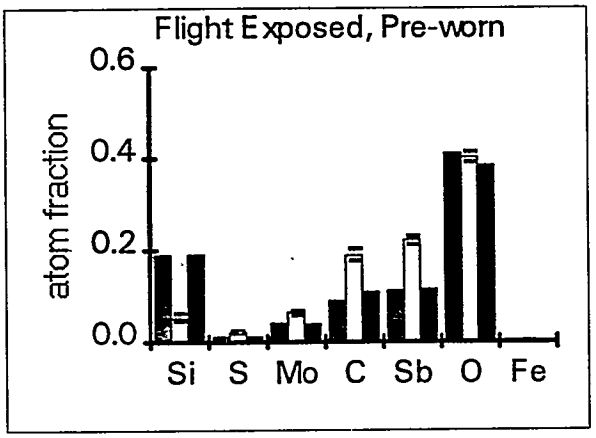

(c)

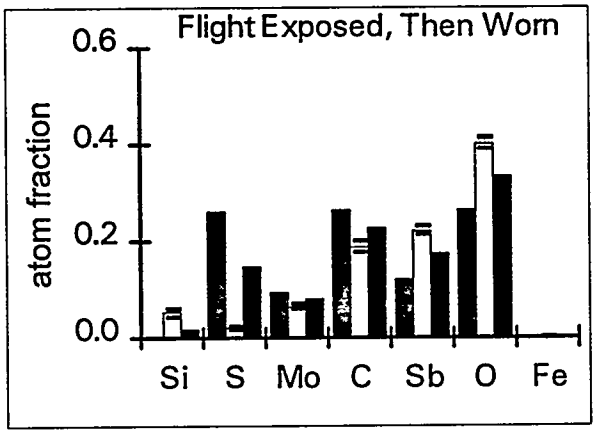

(d)

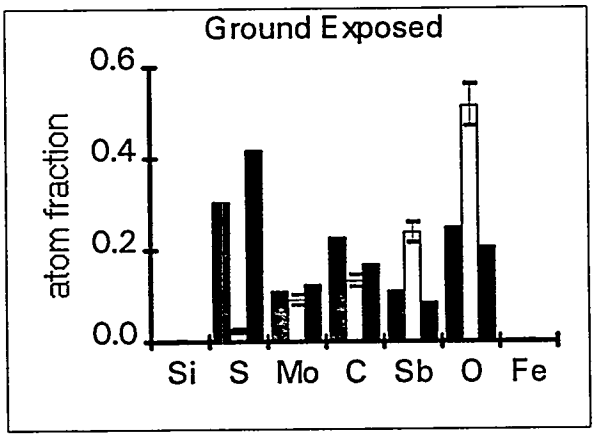

(e)

$MoS_2 + SbO_x$

Figure 7

DISCLAIMER